and u and v are equal to

$$v^2 = [(1 + 4ABt^2)^{1/2} - 1]/2A,$$
$$u^2 = [(1 + 4ABt^2)^{1/2} + 1]/2B. \quad (30)$$

The optimal α and β values can be calculated then as

$$\alpha = v/u, \quad \beta = 1/u^2. \quad (31)$$

A2. Mathematical analysis

We exclude from the analysis the singular case when there exists a scale factor λ such that $F_j^{obs} = \lambda F_j^{mod}$ for all the reflections, *i.e.* the model is ideal.

The function $G(t)$ is even, so we can consider it for $t \geq 0$ only.

It is easy to see that $G(t) = 0$ always has the trivial solution $t = 0$, *i.e.* $v = 0$, $u = B^{-1/2}$ or $\alpha = 0$, $\beta = B$.

Using asymptotic formulae for the modified Bessel functions, we can obtain, for small values of t,

$$G(t) = -2(D - AB)t^2 + O(t^4) \quad \text{for } t \to 0 \quad (32)$$

and, for large t,

$$\lim_{t\to\infty}(1/t)G(t) = 2[(AB)^{1/2} - C]. \quad (33)$$

The value of $(AB)^{1/2} - C$ is always positive owing to Cauchy inequality, so $G(t) = 0$ has at least one nontrivial solution if the value

$$\Omega = D - AB \quad (34)$$

is positive.

It is possible to show, too, that the function $Q(u, v)$ tends to $-\infty$ when the point (u, v) tends to infinity. So, the maximum value is attained at an inner point.

In the vicinity of $u = B^{-1/2}$, $v = 0$,

$$Q(u, v) = (-\ln B - 1) - 2B(u - B^{-1/2})^2 + (\Omega/B)v^2 + \ldots, \quad (35)$$

so if $\Omega < 0$ this point is the maximum point, but if $\Omega > 0$ this is a saddle point and the maximum is attained at a point corresponding to the nontrivial solution of $G(t) = 0$.

References

AGARWAL, R. C. & ISAACS, N. W. (1977). *Proc. Natl Acad. Sci. USA*, **74**, 2835–2839.
BRICOGNE, G. (1984). *Acta Cryst.* A**40**, 410–445.
BRICOGNE, G. (1988). *Acta Cryst.* A**44**, 517–545.
BRICOGNE, G. (1990). *Acta Cryst.* A**46**, 284–297.
BRICOGNE, G. (1993). *Acta Cryst.* D**49**, 37–60.
BRÜNGER, A. T. (1992). *Nature (London)*, **355**. 472–474.
BRÜNGER, A. T. (1993). *Acta Cryst.* D**49**, 24–36.
COX, D. R. & HINKLEY, D. V. (1974). *Theoretical Statistics*. Imperial College, London, England.
LAMZIN, V. S. & WILSON, K. S. (1993). *Acta Cryst.* D**49**, 129–147.
LUNIN, V. YU. (1982). *The Use of Maximum Likelihood Approach to Estimate Phase Errors in Protein Crystallography*. Pushchino, Russia.
LUNIN, V. YU., LUNINA, N. L., PETROVA, T. E., VERNOSLOVA, E. A., URZHUMTSEV, A. G. & PODJARNY, A. (1995). *Acta Cryst.* Submitted.
LUNIN, V. YU. & URZHUMTSEV, A. G. (1984). *Acta Cryst.* A**40**, 269–277.
LUNIN, V. YU., URZHUMTSEV, A. G., VERNOSLOVA, E. A., CHIRGADZE, YU. N., NEVSKAYA, N. A. & FOMENKOVA, N. P. (1985). *Acta Cryst.* A**41**, 166–171.
LUZZATI, V. (1952). *Acta Cryst.* **5**, 802–810.
READ, R. J. (1986). *Acta Cryst.* A**42**, 140–149.
READ, R. J. (1990). *Acta Cryst.* A**46**, 900–912.
SIM, G. A. (1959). *Acta Cryst.* **12**, 813–815.
SRINIVASAN, R. & PARTHASARATHY, S. (1976). *Some Statistical Applications in X-ray Crystallography*. Oxford: Pergamon Press.
SUBBIAH, S. (1991). *Science*, **252**, 128–133.
URZHUMTSEV, A. G., LUNIN, V. YU. & VERNOSLOVA, E. A. (1989). *J. Appl. Cryst.* **22**, 500–506.
WILSON, C. & AGARD. D. A. (1993). *Acta Cryst.* A**49**, 97–104.

Acta Cryst. (1995). A**51**, 887–897

The Analytical Calculation of Absorption in Multifaceted Crystals

BY R. C. CLARK

Department of Mathematical Sciences, University of Aberdeen, Aberdeen AB9 2TY, Scotland

AND J. S. REID

School of Physics, University of Aberdeen, Aberdeen AB9 2UE, Scotland

(*Received* 20 *April* 1995; *accepted* 5 *June* 1995)

Abstract

The exact analytic method of evaluating the absorption during scattering in multifaceted convex crystals is developed in a way that permits efficient computation. A fast and accurate algorithm is given for finding the Howells polyhedra whose determination is fundamental to the analytic method. The algorithm allows for the evaluation of cases when the sample is only partly illuminated, can be adapted to more general situations

and can be used to generate an estimate of the error in the computation. In most cases this is to 1 part in 10^{14}. Results of standard tests are given to greater accuracy than previously available and results for multifaceted approximations to a cylinder and a sphere are given to illustrate the power of the method.

Introduction

The method described here for calculating absorption during scattering has been developed for X-ray scattering by polyhedral single-crystal samples. It applies equally, however, to any homogeneous material whether amorphous or crystalline, to elastic neutron scattering from moderately sized samples or to other weak scattering processes. Moreover, since a cylinder or sphere can be approximated by a many-sided polyhedron, the method can also be used to give results for these and other shapes that are not intrinsically polyhedral.

Although the mathematical techniques have general applicability, it is in the context of X-ray scattering that attempts have been made for over forty years to solve the problem of the calculation of absorption during scattering. The most popular method of calculation is to use Gaussian integration over a three-dimensional grid (Busing & Levy, 1957). This method is not particularly rapid with fine sampling and only achieves good accuracy for small absorption coefficients, μ. With a large absorption coefficient, much of the absorption comes from only a small part of the total sample volume, which is consequently inadequately covered by a Gaussian grid of workable density spread over the whole sample.

It was pointed out by Howells (1950) that the absorption could be calculated analytically for a two-dimensional polygonal crystal. Howells's method was not particularly suited to implementation by computer but the areas into which the crystal was divided became known as Howells polygons and, by extension, the corresponding volumes in three dimensions became known as Howells polyhedra. Howells's two-dimensional division of a crystal formed the basis of the method described by Braibanti & Tiripicchio (1965) but their division of a three-dimensional sample into two-dimensional slices was immediately superseded by a full three-dimensional treatment by de Meulenaer & Tompa (1965). This treatment, involving the subdivision of the Howells polyhedra into tetrahedra, has been the basis of all subsequent work, including that by Alcock (1970, 1974) and Blanc, Schwarzenbach & Flack (1991). It has been used in comparisons between analytical evaluations and numerical methods, notably by Alcock (1974) and Flack, Vincent & Alcock (1980).

Clark (1993) reconsidered the calculation of the absorption *ab initio* and established a formula for the evaluation of the transmission factor dependent only on the edges of the Howells polyhedra. In this paper, the methods described by Clark are analysed in greater detail and computational considerations included. In order to maintain high accuracy, we pay particular attention to the special cases where the denominators in Clark's formula tend to zero. It turns out that the simplest way of dealing with these special cases is to use expansion formulae similar to those worked out by Blanc, Schwarzenbach & Flack (1991). The links between the two methods are established in the next section.

In this paper, we use the method suggested by Clark (1993) of defining the Howells polyhedra in terms of the included volume within a given set of planes. We develop this concept and show how it can be used to generate the Howells polyhedra rapidly and simply. Any exact computational method requires the finding of the vertices and edges of each Howells polyhedron and it is this time-consuming process that causes exact calculations to be underused. A special algorithm has been devised that steps sequentially around the edges of each of the polyhedra and evaluates the appropriate contribution to the transmission coefficient and other formulae as each edge is found. The process is made efficient by minimizing the number of planes required to define each polyhedron and also by minimizing the number of polyhedra that have to be checked. In the second section of this paper, the computational method is described.

We believe that the speed and accuracy of the process described here tips the balance strongly in favour of exact calculation of X-ray (and other) absorption factors.

Mathematical analysis

The transmission factor T of a convex polyhedral crystal completely bathed in X-rays is defined by

$$T = V^{-1} \int_V \exp(-\mu L)\, \mathrm{d}V, \tag{1}$$

where the crystal volume V is subdivided into Howells polyhedra. The subdivision of a crystal into Howells polyhedra (see Fig. 1) is a division into volumes within which the total path length L of the ray scattered at a point with coordinates $\mathbf{r}$ varies linearly with position. Thus, within any Howells polyhedron, $L(\mathbf{r})$ obeys the general relation

$$L(\mathbf{r}) = \mathbf{a} \cdot \mathbf{r} + c, \tag{2}$$

where $\mathbf{a}$ is a constant vector and c a scalar constant. [For any particular polyhedron, the values of $\mathbf{a}$ and $\mathbf{c}$ can be deduced from equation (14) below.]

Clark (1993) showed how to reduce the integral over each Howells polyhedron to a sum over its edges by using Gauss's and Stokes's theorems. The method Clark described can be applied to integrals of any function of L over polyhedral volumes. In effect, Clark established the result that, if $\psi(L)$ is any thrice differentiable function

of L and V is a volume within which (2) holds, then

$$\int_V (\mathrm{d}^3\psi/\mathrm{d}L^3)\,\mathrm{d}V = \sum_{k,j} a^{-2}[(\mathbf{n}_k \cdot \mathbf{a})/|\mathbf{n}_k \times \mathbf{a}|^2] \times [\mathbf{n}_k, \mathbf{a}, \mathbf{d}_j](\psi_{j+1} - \psi_j)/(\mathbf{a} \cdot \mathbf{d}_j). \quad (3)$$

The sum over k is over all faces of the polyhedron and the sum over j is taken over all edges of each face. The vector $\mathbf{n}_k$ is the unit vector normal to face k. We have written ψ_j for $\psi(L(\mathbf{r}_j))$, the value of ψ at $\mathbf{r}_j$, and numbered the vertices so that $\mathbf{r}_j$ and $\mathbf{r}_{j+1}$ are the position vectors of the vertices at the beginning and the end of edge j, respectively. The symbol [a, b, c] is the triple scalar product $\mathbf{a} \times \mathbf{b} \cdot \mathbf{c}$, $a = |\mathbf{a}|$ and the vector $\mathbf{d}_j$ is defined by $\mathbf{d}_j = \mathbf{r}_{j+1} - \mathbf{r}_j$. In the usual way, all edges round a face are traversed anticlockwise round the outward going normal, $\mathbf{n}_k$, to that face. We note that $\mathbf{a} \cdot \mathbf{d}_j$is the difference between the values of L at the ends of edge j.

The cases when $|\mathbf{n}_k \times \mathbf{a}|$, $|\mathbf{a}|$ or $\mathbf{a} \cdot \mathbf{d}_j$ are small but non-zero require special evaluation. The last two of these can easily be handled by a Taylor-series expansion but the first requires more careful analysis. Blanc, Schwarzenbach & Flack (1991) have shown how to treat the equivalent situation that occurs when path lengths through the vertices of a tetrahedron become equal. Establishing the connection between their method and our equation (3) gives insight into both formulae and leads to a form that is simple to use. Hence we now show how to remove the cross product from the denominator of equation (3).

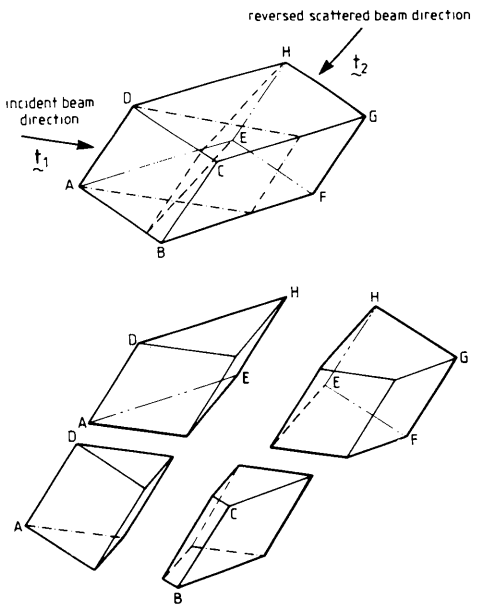

Fig. 1. The incident beam illuminates the crystal along direction $\mathbf{t}_1$ through faces *ABCD* and *ADHE*. Scattered radiation leaves in the direction $-\mathbf{t}_2$ through faces *EFGH* and *ADHE*. The transmission factor T for a convex polyhedral sample is evaluated by dividing the sample into Howells polyhedra, for each of which the incident beam and the reversed scattered beam enter the sample through a single face. The shape illustrated is divided into four Howells polyhedra, shown in exploded view below.

We can rewrite (3) as

$$\int_V (\mathrm{d}^3\psi/\mathrm{d}L^3)\,\mathrm{d}V = \sum_k a^{-2}[(\mathbf{n}_k \cdot \mathbf{a})/|\mathbf{n}_k \times \mathbf{a}|^2](\mathbf{n}_k \times \mathbf{a}) \cdot \left[\sum_j \mathbf{d}_j(\psi_{j+1} - \psi_j)/(\mathbf{a} \cdot \mathbf{d}_j)\right]. \quad (4)$$

The sum round the edges of the polygon in the final bracket can be re-expressed as

$$\sum_j \psi_j[\mathbf{d}_{j-1}/(\mathbf{a} \cdot \mathbf{d}_{j-1}) - \mathbf{d}_j/(\mathbf{a} \cdot \mathbf{d}_j)] = \sum_j \{\psi_j/[(\mathbf{a} \cdot \mathbf{d}_j)(\mathbf{a} \cdot \mathbf{d}_{j-1})]\}\mathbf{a} \times (\mathbf{d}_{j-1} \times \mathbf{d}_j). \quad (5)$$

But $\mathbf{d}_{j-1} \times \mathbf{d}_j = (\mathbf{n}_k \cdot \mathbf{d}_{j-1} \times \mathbf{d}_j)\mathbf{n}_k$ since all the edges lie in the plane with normal $\mathbf{n}_k$. Hence,

$$\int_V (\mathrm{d}^3\psi/\mathrm{d}L^3)\,\mathrm{d}V = -\sum_{k,j} a^{-2}\mathbf{n}_k \cdot \mathbf{a}[\mathbf{n}_k, \mathbf{d}_{j-1}, \mathbf{d}_j] \times [\psi_j/(\mathbf{a} \cdot \mathbf{d}_j)(\mathbf{a} \cdot \mathbf{d}_{j-1})]. \quad (6)$$

Expression (6) has eliminated the awkward denominator $|\mathbf{n}_k \times \mathbf{a}|$ but at the expense of introducing a sum over vertices rather than edges and requiring the evaluation of two vectors $\mathbf{d}_j$ and $\mathbf{d}_{j-1}$ meeting at that vertex. It is computationally convenient to retain the evaluation of the sum edge by edge. To do this, on each face k we define a reference point $\mathbf{r}_k$ and observe that the sum round the polygon on that face can be re-expressed as a sum over triangles whose vertices are at $\mathbf{r}_k$, $\mathbf{r}_j$ and $\mathbf{r}_{j+1}$ (Fig. 2).

Let $\mathbf{s}_j$ be defined for each vertex by $\mathbf{s}_j = \mathbf{r}_j - \mathbf{r}_k$. Round each triangle, the triple scalar product in (6) has a constant value because, as $\mathbf{d}_j = \mathbf{s}_{j+1} - \mathbf{s}_j$, we have

$$[\mathbf{n}_k, \mathbf{s}_j, \mathbf{d}_j] = [\mathbf{n}_k, \mathbf{d}_j, -\mathbf{s}_{j+1}] = [\mathbf{n}_k, -\mathbf{s}_{j+1}, \mathbf{s}_j] = [\mathbf{n}_k, \mathbf{s}_j, \mathbf{s}_{j+1}]. \quad (7)$$

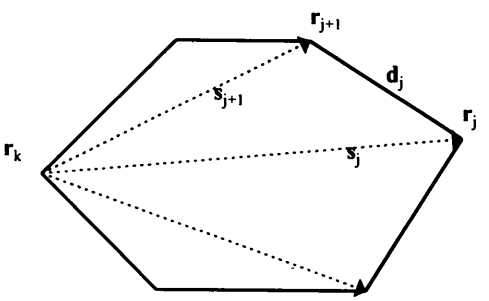

Fig. 2. Each polygonal face of a Howells polyhedron can be divided into a set of triangles with one vertex at $\mathbf{r}_k$. Note that $\mathbf{s}_j \times \mathbf{s}_{j+1}$ is zero if either $\mathbf{r}_j$ or $\mathbf{r}_{j+1}$ is equal to $\mathbf{r}_k$.

Also, since both $\mathbf{s}_j$ and $\mathbf{s}_{j+1}$ lie in the plane with normal $\mathbf{n}_k$, it follows that

$$\mathbf{n}_k \cdot \mathbf{a}[\mathbf{n}_k, \mathbf{s}_j, \mathbf{s}_{j+1}] = [\mathbf{a}, \mathbf{s}_j, \mathbf{s}_{j+1}]. \quad (8)$$

Defining $L_k = L(\mathbf{r}_k)$ and using $\mathbf{a} \cdot \mathbf{d}_j = L_{j+1} - L_j$ *etc.*, we have the following expression for the integral.

$$\begin{aligned}\int_V (\mathrm{d}^3\psi/\mathrm{d}L^3)\,\mathrm{d}V &= \sum_{k,j} a^{-2}[\mathbf{a}, \mathbf{s}_j, \mathbf{s}_{j+1}] \\ &\times \{[\psi_k/(L_k - L_j)(L_k - L_{j+1})] \\ &+ [\psi_j/(L_j - L_k)(L_j - L_{j+1})] \\ &+ [\psi_{j+1}/(L_{j+1} - L_k)(L_{j+1} - L_j)]\}. \quad (9)\end{aligned}$$

We have now established the link between our formulae and those of Blanc, Schwarzenbach & Flack (1991). Equation (9) is closely related to their equation (11). The differences are that (9) is an expression that can be used with a general $\psi(L)$ and, perhaps more importantly, our expression requires no tetrahedron to be defined. It has been necessary in going from (3) to (9) to choose a special point, $\mathbf{r}_k$, on each plane but this is simply a book-keeping exercise. The rest of the Howells polyhedron does not need to be known when calculating the contribution from any edge.

It is tempting to let $\mathbf{r}_k$ be the end of the normal vector from the origin onto plane k. This would simplify the computations but we note that L will have to be evaluated at $\mathbf{r}_k$. It is sensible to take $\mathbf{r}_k$ within or on the polygon on face k since then L_k will have a physically meaningful value. In this way, excessively large values of ψ are avoided and rounding errors minimized. In practice, we use the first vertex found on each face as $\mathbf{r}_k$.

Evaluation of the final bracketed term in (9) in the cases when the denominators are small can be carried out as described in the Appendix to Blanc, Schwarzenbach & Flack (1991). Building on the earlier work of de Meulenaer & Tompa (1965) and Alcock (1970), they show how Taylor-series expansions about an appropriately chosen point can be used. We use the centre point of edge j when $L_{j+1} - L_j$ is small, as the expansion then only requires even powers. As noted in earlier papers, the bracketed term in (9) is symmetric under interchanges of L_k, L_j, L_{j+1} so that if these are ordered in increasing order as L_1, L_2, L_3 then the term within curly brackets can be rewritten as

$$(L_3 - L_1)^{-1}[(\psi_3 - \psi_2)/(L_3 - L_2) - (\psi_2 - \psi_1)/(L_2 - L_1)]. \quad (10)$$

When L_1, L_2 and L_3 are all approximately equal, this makes the expansion about the intermediate value, L_2, particularly transparent.

The case of small $|\mathbf{a}|$ can be treated by a Taylor-series expansion about $L = c$ and the case of small μ, the absorption coefficient, by expanding about $\mu = 0$. Convergence is verified in each case by checking that the first omitted term is less than 10^{-18} of the first term. Some mathematical details are given in Appendix 2. We have not found it necessary to use the expression for $\psi(L)$ suggested by Clark (1993) in his equation (31). Instead, we use the following functions:

for the transmission factor,

$$\psi(L) = \exp(-\mu L)/(-\mu)^3; \quad (11a)$$

for its derivative with respect to μ,

$$\psi(L) = (\mu L + 3)\exp(-\mu L)/(-\mu)^4; \quad (11b)$$

for the volume of any polyhedron,

$$\psi(L) = L^3/6; \quad (11c)$$

for area integrals of $\exp(-\mu L)$,

$$\psi(L) = \exp(-\mu L)/(-\mu)^2. \quad (11d)$$

Blanc, Schwarzenbach & Flack (1991) describe how to calculate the derivatives of the transmission factor with respect to the positions of the crystal face planes. The inclusion of the calculation of these derivatives is, as they point out, easily incorporated in any computer program as many of the relevant quantities have already been evaluated. It can be seen directly from (9) that the equivalent result for area integrals over polygons is

$$\begin{aligned}\int_S (\mathrm{d}^2\psi/\mathrm{d}L^2)\,\mathrm{d}S = \sum_j [\mathbf{n}, \mathbf{s}_j, \mathbf{s}_{j+1}] \\ \times \{[\psi_k/(L_k - L_j)(L_k - L_{j+1})] \\ + [\psi_j/(L_j - L_k)(L_j - L_{j+1})] \\ + [\psi_{j+1}/(L_{j+1} - L_k)(L_{j+1} - L_j)]\} \quad (12)\end{aligned}$$

and hence virtually no extra calculation is required to evaluate the derivatives other than the use of (11*d*) for ψ. It is also straightforward to evaluate the mean path length in the crystal, $\overline{T}$, from the formula (Zachariasen, 1967)

$$\overline{T} = -(1/T)(\partial T/\partial \mu). \quad (13)$$

Computational errors and limitations on the accuracy of the method

Computational errors may be detected by comparing the volumes of the Howells polyhedra calculated in two different ways. Firstly, the volume of any polyhedron may be found algebraically from its enclosing planes and, secondly, by using (9) and integrating over $L^3/6$. We emphasize that no short cuts need be taken in this second calculation. Exactly the same steps are

made to integrate $L^3/6$ as are used to evaluate the transmission-factor integrals. Every factor required in one calculation is also required in the other. The only difference being the use of (11*c*) instead of (11*a*). The very small differences that typically exist between the two evaluations of the volume permit confidence in the evaluation of all other integrals and in the estimated errors. In normal situations, the volume of each Howells polyhedron obtained by integration is extremely close to that obtained algebraically from its defining planes – typically to 1 part in 10^{14}. Similarly, only exceptionally is the difference between the volume of the crystal obtained directly and the volume obtained by summing the volumes of the Howells polyhedra other than very small. This difference is usually at the limits of the accuracy achievable, allowing for rounding errors on double-precision variables. This implies that, for small μ, the transmission factor will be calculated to the same order.

Where errors are found, it is because it is occasionally necessary to subtract two large numbers when finding the vertices of the Howells polyhedra. Such a subtraction occurs when the cross product of two nearly parallel vectors is required. The subsequent rounding errors may be crucial when determining whether a small quantity is zero or not. For this reason, the search algorithm may fail to find all the vertices of very thin or very narrow Howells polyhedra. All such polyhedra are regarded as of zero volume (*i.e.* eliminated because they fail Euler's relation) when in fact some may have a small but finite size. Such flat or thin polyhedra are liable to occur very close to special symmetry orientations of the crystal in the incident beam or close to special scattering angles. Fortunately, the double calculation of the crystal volume allows their omission to be readily identified and the error estimated. One way of avoiding these errors is to make a small change in the crystal setting angles or in the scattering angle. Because the errors arise from rounding, a small change in the input data, usually as small as a few thousandths of a degree, will remove the error condition and restore accurate results.

A second limitation on the accuracy arises from the calculation of the path length through the crystal. The total path length through $\mathbf{r}$ along an incident-beam direction $\mathbf{t}_1$ and a (reversed) scattered-beam direction $\mathbf{t}_2$ between two faces described by $\mathbf{n}_1$, D_1 and $\mathbf{n}_2$, D_2 (when $\mathbf{n}\cdot\mathbf{r} - D = 0$ is the equation of a plane) is

$$L = -(\mathbf{n}_1\cdot\mathbf{r} - D_1)/(\mathbf{n}_1\cdot\mathbf{t}_1) - (\mathbf{n}_2\cdot\mathbf{r} - D_2)/(\mathbf{n}_2\cdot\mathbf{t}_2) \quad (14)$$

and either of the denominators $\mathbf{n}_1\cdot\mathbf{t}_1$ or $\mathbf{n}_2\cdot\mathbf{t}_2$ may be very small. This means that there can be significant multiplication of the rounding error on $\mathbf{r}$. This limitation on the accuracy applies, of course, to all methods of calculating the transmission factor. It is most acute when the absorption coefficient is large as then the factor will depend mostly on a few path lengths near the incident face. We have not been able to escape from this limitation. We note, however, that, in the configurations when it occurs, discrepancies between the real geometry of the crystal and the modelled geometry will have a much greater effect than normal.

An estimate of the error in the transmission factor can be made by summing the difference in the two methods of calculating the volume of each Howells polyhedron weighted by $\exp(-\mu L_{\min})$, where $L_{\min}$ is the minimum path length to the polyhedron. In our calculation, we add to this estimate the difference between the total crystal volume and the sum of the volumes of the Howells polyhedra. This flags any omitted polyhedra. The total, divided by the volume of the crystal, is given in the tables in the final section as the estimated error.

Generation of the Howells polyhedra

Despite the fact that the analytic procedure described above is simpler to implement than earlier methods, it is the time-consuming process of finding the vertices of the Howells polyhedra that makes the evaluation of the transmission factor and its derivatives of limited use for crystals with more than 20 faces. By giving careful attention to several aspects of the search strategy for the Howells polyhedra and their vertices, we have been able to increase the computing speed by orders of magnitude for large many-faceted crystals. For clarity in what follows, we will refer to the Howells polyhedron lit by the incident beam through face *A* and also lit by the (reversed) scattered beam through face *B* as polyhedron [*A*,*B*] or as having indices *A*,*B*.

The set of planes required to define each Howells polyhedron consists of the face planes of the crystal and two sets of 'lit-edge' planes. A lit-edge plane is the projection of a lit edge of the crystal along the relevant X-ray direction. The two sets required are the lit-edge planes parallel to the incident beam that outline face *A*, set (*a*), and the set of lit-edge planes parallel to the (reversed) scattered-beam direction that outline face *B*, set (*b*) (see Fig. 3). We will refer to the crystal face planes as set (*c*).

Many of the planes in the combined set (*a*), (*b*), (*c*) will lie completely outside the desired included volume. It is important to reduce the number in the defining set to a minimum, since any intersection of triples of planes in the set is a possible vertex of the included volume. The number of such points increases as the cube of the number of planes. While not all these points are tested in the procedure explained below, it is clearly sensible to eliminate any unnecessary planes from the set. We note that, of all the crystal faces lit by the incident beam, only one need be included – namely the one that defines the Howells polyhedron, face *A*. Even this one need not be included if it is lit by the scattered beam and index *B* is not equal to *A*. Similarly, at most only one crystal

face lit by the scattered beam need be included, face B, and even this need not be included in many cases. Hence, the number of crystal face planes required in set (c) is just the number of faces unlit by either beam plus zero, one or two. Similar considerations can be applied to the lit-edge planes around faces A and B, sets (a) and (b) above. No such plane need be included unless the crystal edge it passes through lies between two crystal faces both of which are lit by the same beam (Alcock, 1970). If a single lit edge generates two lit-edge planes, a simple calculation determines whether one or both are required.

Having reduced the set of planes as much as possible, an initial vertex has to be located. This is found by evaluating $\mathbf{n} \cdot \mathbf{r} - D$ for all other planes in the set when $\mathbf{r}$ is the point of intersection of three of them. The first points searched should be the intersections of lit-edge planes as the most likely planes to form a vertex of the polyhedron. Indeed, if any lit-edge planes intersect the body of the crystal then at least one face of the Howells polyhedron must lie on one of them. This fact enables us to reduce the search path for the first vertex considerably and speeds up the elimination of sets of planes that cannot generate Howells polyhedra within the crystal.

The following algorithm finds the vertices of a polyhedron defined by a set of planes, by stepping from one vertex to another round the edges until the whole polyhedron is encompassed. The basic method is fast and robust for simple sets of planes. We also describe how to deal with the complications that can arise when there are planes that are tangential to the included volume through one of its edges or through one of its vertices.

Once a vertex, $\mathbf{r}_1$, has been found, all planes passing through $\mathbf{r}_1$ are listed and ordered round the vertex. The method of ordering is explained in Appendix 1. Also explained in Appendix 1 is how planes tangent to the Howells polyhedron at this vertex can be eliminated from the set. Neighbouring pairs of planes passing through a vertex define the edges through that vertex. Each edge can be labelled uniquely by the (ordered) numbers of the pair of planes passing through it. These labels are passed to an edge list together with the number of the vertex $\mathbf{r}_1$, while $\mathbf{r}_1$ is itself recorded. A second vertex is now sought for the first edge on the edge list by searching for that plane whose intersection (at $\mathbf{r}_2$) with the edge is the closest to the vertex $\mathbf{r}_1$. This involves only one pass through the set of planes. Once both ends of an edge have been found, its contribution to the integrals can be calculated and it can be eliminated from the edge list.

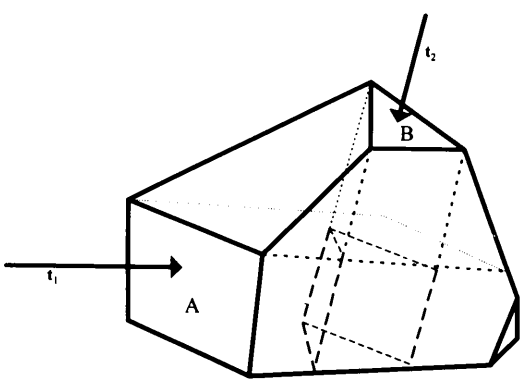

Fig. 3. Any Howells polyhedron can be defined by the set of planes made up of the lit-edge planes of face A, the lit-edge planes of face B, the unlit faces of the crystal plus, at most, face A and face B.

The new vertex, $\mathbf{r}_2$, is now treated in the same way as $\mathbf{r}_1$. All planes through it are found and new edges generated and added to the edge list. The edge list is checked for duplicates, since duplication indicates that both ends have been found. These completed edges are then processed and removed from the edge list. The procedure then repeats until the edge list is empty and, hence, all vertices found.

This method reduces to a minimum the number of points that have to be tested as vertices of the polyhedron. Apart from the first vertex, which involves a search that might in principle increase in proportion to p^3, where p is the number of planes in the set, all other searches are in proportion to p. Clark (1993) estimated that the number of planes in parts (a) and (b) of the set will be about 12, on average, and we have shown above that the number required from part (c) is the number of unlit crystal faces plus, at most, two.

Computing speed can also be greatly increased by listing neighbouring Howells polyhedra whenever one is found and subsequently stepping directly to these known polyhedra. This can be done by recording the index number of the neighbouring face whenever any lit-edge plane is generated. Then the indices of the neighbouring polyhedra to polyhedron $[A,B]$ can be deduced from the fact that any edge of polyhedron $[A,B]$ that is the intersection of two lit-edge planes must be common to three neighbouring Howells polyhedra. Similarly, any edge that is the intersection of a lit-edge plane and a crystal face is an edge of one other Howells polyhedron. By stopping searching for more Howells polyhedra when the total volume of the crystal has been found, very few sets of planes that do not contain Howells polyhedra need be generated.

We note finally that if the data relevant to each edge are stored for any crystal orientation, no recalculation of the Howells polyhedra is required if only μ is changed. Very rapid computation of the transmission factor as a function of μ can be produced for each orientation, a feature that is particularly useful in energy-dispersive experiments (Reid, 1993).

Partly illuminated crystals

Since the routine uses a set of planes to describe the crystal and its associated Howells polyhedra, it is a simple matter to include in the set of planes any that

define the limits of the illuminating beam. These reduce the number of Howells polyhedra that contribute to the absorption but do not change the path lengths L to any vertex. The path lengths are still determined by the total length of a ray between a crystal face lit by the incident beam and one lit by the scattered beam. The facility to include explicitly these 'beam planes' in the calculation of the absorption factor means that crystal mounting faces, for example, can be excluded. Scattering in one small part of a sample can also be studied.

The inclusion of beam planes means that the definition of the transmission factor needs to be slightly modified. We redefine T to be

$$T = v^{-1} \int_v \exp(-\mu L)\, \mathrm{d}v, \qquad (15)$$

where v is that volume of the crystal in which scattering occurs. As remarked above, this definition does not affect the definition of the path length L or any of the mathematical analysis above. All that needs to be changed is the volume over which the integral is taken.

This concept of scattering occurring in only a small part of the volume could be extended to more complex situations. The derivation of (9) depends only on the fact that L is linearly dependent on $\mathbf{r}$ within any Howells polyhedron. Thus, the theory could readily be extended to convex polyhedral crystals with one absorption coefficient contained within other convex polyhedra with different absorption. The expression for μL in the case of a crystal with absorption coefficient μ_1 inside an absorbing medium with absorption coefficient μ_2 would be changed from

$$\mu(\mathbf{a} \cdot \mathbf{r} + c)$$

to

$$\mu_2(\mathbf{a}_2 \cdot \mathbf{r} + c_2) + (\mu_1 - \mu_2)(\mathbf{a}_1 \cdot \mathbf{r} + c_1), \qquad (16)$$

where $\mathbf{a}_1$, c_1 are defined by the crystal planes in the usual way and $\mathbf{a}_2$, c_2 are defined in a similar manner by the outer polyhedron planes. Each Howells polyhedron would then be defined by four indices instead of two but this would present no computational problem, since it would merely increase the number of planes in the set defining the polyhedron. The use of beam planes to focus on the region of interest would eliminate unnecessary computations.

Tests

We present tests of three types. First, analytic formulae for simple shapes against which any program can be tested. These are useful in the initial stages of preparation of computer programs but usually do not serve as complete tests because the number of Howells polyhedra is necessarily limited. However, the formulae given below are more generally applicable than earlier formulae (Cahen & Ibers, 1972) in that they allow for a wide range of polyhedral shapes, scattering angles and scattering directions. Secondly, we give a set of results for Alcock's standard irregular crystal (Alcock, 1974) to extended accuracy. We give results for the derivatives of the transmission factor with respect to the positions of the face planes calculated both numerically and analytically (Blanc, Schwarzenbach & Flack, 1991) and finally results for polyhedral approximations to a cylinder and sphere to illustrate the power of the method.

Clark (1993) published an analytic formula for the transmission factor applicable to any tetrahedron oriented so that it is a single Howells polyhedron with both the incident and scattered beams passing through the same face. That result is

$$T_1(L) = 6(\mu L)^{-3}[1 - \mu L + \tfrac{1}{2}\mu^2 L^2 - \exp(-\mu L)], \qquad (17)$$

where L is the path length of the ray scattered at the 'hidden' vertex (see Fig. 4*a*). This formula will

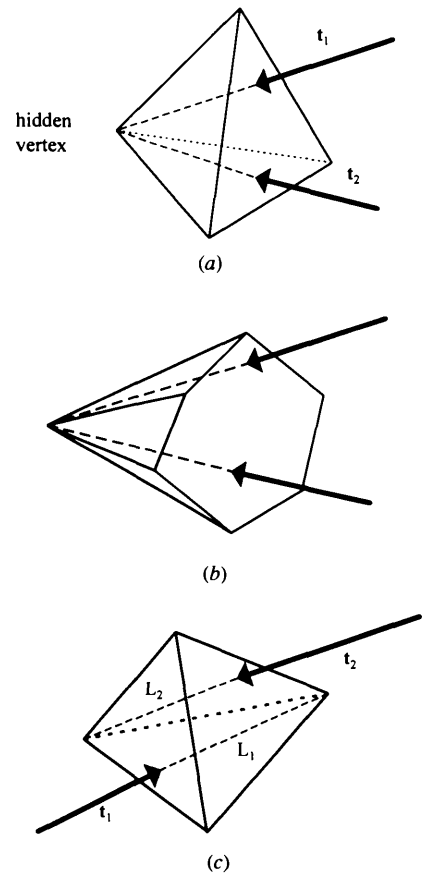

Fig. 4. (*a*) A tetrahedron illuminated through a single face. The total path length L to the hidden vertex is shown dashed. The transmission coefficient is given by equation (17) in this configuration. (*b*) A polyhedron whose transmission coefficient is also given by equation (17). (*c*) A tetrahedron with two faces illuminated showing the path lengths L_1 and L_2 to either end of the hidden edge. Equation (18) applies in this case.

also apply to polyhedra of any shape which can be decomposed into tetrahedra satisfying the geometrical constraints (Fig. 4*b*).

It is not difficult to see that the equivalent formula for a tetrahedron which again is a single Howells polyhedron but where the incident and scattered beams pass through different faces is

$$T_2 = [L_1T_1(L_1) - L_2T_1(L_2)]/(L_1 - L_2), \qquad (18)$$

where L_1 and L_2 are the path lengths of the two rays passing through the ends of the 'hidden' edge (Fig. 4*c*). This formula can also be written as the ratio of two determinants:

$$\begin{vmatrix} 1 & L_1T_1(L_1) \\ 1 & L_2T_1(L_2) \end{vmatrix} \Big/ \begin{vmatrix} 1 & L_1 \\ 1 & L_2 \end{vmatrix} \qquad (19)$$

and, while there are no other ways that an isolated tetrahedron can be a single Howells polyhedron, an obvious extension to four path lengths gives de Meulenaer & Tompa's (1965) original tetrahedron formula in the form

$$\begin{vmatrix} 1 & L_1 & L_1^2 & L_1^3T_1(L_1) \\ 1 & L_2 & L_2^2 & L_2^3T_1(L_2) \\ 1 & L_3 & L_3^2 & L_3^3T_1(L_3) \\ 1 & L_4 & L_4^2 & L_4^3T_1(L_4) \end{vmatrix} \Big/ \begin{vmatrix} 1 & L_1 & L_1^2 & L_1^3 \\ 1 & L_2 & L_2^2 & L_2^3 \\ 1 & L_3 & L_3^2 & L_3^3 \\ 1 & L_4 & L_4^2 & L_4^3 \end{vmatrix}. \qquad (20)$$

It is easy to check that (17) and (18) are reproduced by any numerical program for all scattering angles within the given geometrical constraints. Our program satisfies this test.

Alcock (1974) published a set of test results for an irregular crystal. We reproduce our calculation for this crystal in Table 1 and extend the test to both low and high values of μ. We have given our results to ten decimal places because we believe for such a simple crystal they are accurate to at least that figure. Double-precision arithmetic with a word length of 64 bits was used throughout the calculations, which took about 15 ms per point on a Sun Sparc 10 CPU running at 50 MHz. We would like to emphasize how useful Alcock's original data are. It is, for example, possible to obtain results – with negligible rounding errors – that are completely erroneous because of an erroneous calculation of the direction of the scattered beam. Cross checks against Alcock's data eliminate this risk.

To enable our data to be cross checked to the accuracy printed, we give the precise values of the scattering angle 2θ and of the angle of rotation of the crystal about the scattering direction ψ (Schwarzenbach & Flack, 1989, 1992). The values of ψ have been taken from Blanc, Schwarzenbach & Flack (1991). The scattering angle used has been chosen to agree with Alcock's results and the unit-cell data and reflection indices also are as given by Alcock. It will be seen from Table 1 that our results for this crystal agree with those found by the program

Table 1. *Computed results for Alcock's irregular crystal; T is the transmission factor and $\bar{T}$ is the mean path length in the crystal*

The estimated error is calculated as described in the text.

Summary of crystal face planes

Plane	Outward normal direction			D
1	1.00	0.00	0.00	1.00
2	0.00	1.00	1.00	1.50
3	0.00	−2.00	1.00	0.50
4	−3.00	0.00	1.00	0.30
5	1.00	1.00	−4.00	1.30

Summary of crystal data

a (Å)	b (Å)	c (Å)	α (°)	β (°)	γ (°)
10.00	11.00	12.00	95.80	101.31	106.80

h	k	l	2θ (°)	ψ (°)	μ	T	$\bar{T}$	Estimated error
0	1	1	12.3620	149.930	0.01	0.9882881407	1.1773349546	0.66D−15
					1.0	0.3348808866	1.0010406886	0.11D−14
					100.0	0.0003296617	0.0118013055	0.26D−14
0	0	1	7.6220	185.550	0.01	0.9883252525	1.1734597148	0.32D−15
					1.0	0.3396683266	0.9784720808	0.12D−14
					100.0	0.0000799667	0.0199348568	0.77D−14
0	0	−1	7.6220	354.450	0.01	0.9883252525	1.1734597148	0.33D−15
					1.0	0.3396683266	0.9784720808	0.35D−15
					100.0	0.0000799667	0.0199348568	0.14D−13
1	2	3	35.7610	179.890	0.01	0.9875170717	1.2550648079	0.90D−15
					1.0	0.3199637261	1.0142173188	0.18D−14
					100.0	0.0006227068	0.0108276575	0.12D−14
1	2	−3	28.0470	37.440	0.01	0.9784782245	2.1717941362	0.16D−14
					1.0	0.1679707070	1.4048239242	0.41D−14
					100.0	0.0000264975	0.0199652043	0.49D−14
1	−2	3	28.0590	174.450	0.01	0.9842463628	1.5856270345	0.33D−15
					1.0	0.2562736811	1.1399579320	0.96D−15
					100.0	0.0000555037	0.0199403609	0.65D−16
1	−2	−3	29.0810	21.850	0.01	0.9882406846	1.1820508162	0.24D−15
					1.0	0.3357461633	0.9926506109	0.23D−14
					100.0	0.0000749679	0.0199384964	0.74D−15
−1	2	3	29.0810	158.150	0.01	0.9882406846	1.1820508162	0.36D−15
					1.0	0.3357461633	0.9926506109	0.14D−14
					100.0	0.0000749679	0.0199384964	0.51D−15
−1	2	−3	28.0590	5.550	0.01	0.9842500235	1.5848828734	0.29D−15
					1.0	0.2658348945	1.0704915076	0.17D−14
					100.0	0.0007922952	0.0105223399	0.23D−14
−1	−2	3	28.0470	142.560	0.01	0.9784829264	2.1708316700	0.82D−15
					1.0	0.1773173018	1.2992022784	0.44D−14
					100.0	0.0005587167	0.0103197667	0.67D−13
−1	−2	−3	35.7610	0.110	0.01	0.9875165229	1.2551761669	0.30D−15
					1.0	0.3174956896	1.0317538530	0.10D−14
					100.0	0.0000678768	0.0199423049	0.46D−15

LSABS (Blanc, Schwarzenbach & Flack, 1991) to the smaller number of decimal places they publish.

Derivatives of the transmission factor with respect to small changes in the position of the crystal face planes may be compared with numerical evaluations of the same derivatives (Blanc, Schwarzenbach & Flack, 1991). When calculating these derivatives, the face planes are assumed to make an outward movement. Hence, numerical increases in D are positive whatever the sign of D (care must be taken if D is zero). We give in Table 2 such a comparison of results for a cylindrical crystal. Beam planes were chosen so that the incident beam illuminates only a slice of the cylinder and the derivatives have been computed using (15) for T. The values of the scattering angle and scattering direction were taken such that the scattered-beam direction is along the axis of the cylinder

Table 2. *The derivatives of T with respect to D_j for each of the crystal faces ($j = 1$ to 8) and for the beam-defining planes ($j = 9, 10$)*

The crystal is defined in Fig. 5. The step size used for the numerical evaluation of the derivatives was 10^{-6} added to the value of D_j for each plane regardless of the sign of D_j.

Summary of crystal face planes

Plane	Outward normal direction			D_j
1	0.0000	0.0000	1.0000	1.0000
2	0.0000	0.0000	−1.0000	1.0000
3	−1.0000	0.0000	0.0000	0.9523
4	−0.5000	−0.8660	0.0000	0.9523
5	0.5000	−0.8660	0.0000	0.9523
6	1.0000	0.0000	0.0000	0.9523
7	0.5000	0.8660	0.0000	0.9523
8	−0.5000	0.8660	0.0000	0.9523

Summary of beam-defining planes

9	0.0000	1.0000	0.0000	−0.8000
10	0.0000	−1.0000	0.0000	0.9000

Summary of crystal data

h	k	l	2θ (°)	ψ (°)	μ	T	$\bar{T}$	Estimated error
1	0	1	90.000	−90.000	1.0	0.077317882	2.4350314	0.15D−14

Plane	Computed $\partial T/\partial D$	Numerical $\partial T/\partial D$
1	−0.77317882D−01	−0.77317843D−01
2	0.00000000D+00	0.22204460D−09
3	−0.18865970D−01	−0.18865957D−01
4	−0.24585404D−02	−0.24585292D−02
5	−0.24585404D−02	−0.24585293D−02
6	−0.18865970D−01	−0.18865957D−01
7	−0.24585404D−02	−0.24585294D−02
8	−0.24585404D−02	−0.24585294D−02
9	0.39303149D−01	0.39303136D−01
10	−0.38014733D−01	−0.38014720D−01

(see Fig. 5). Note that the mean path length, $\overline{T}$, is greater than but roughly equal to the height of the crystal.

Finally, we have computed the absorption of a 100-sided polycylinder and a 74-sided polysphere. Table 3 shows results for the cylinder with the scattering plane perpendicular to the cylinder axis. To the accuracy given, there is no dependence of the calculated absorption

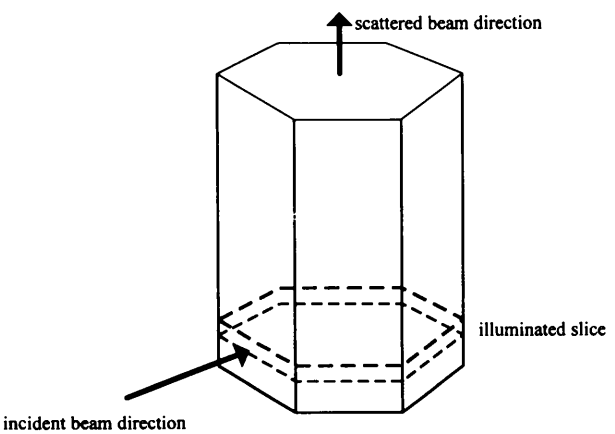

Fig. 5. The hexagonal cylinder used to test the derivatives of T with respect to the face plane distances D_j. The diagram also shows the use of a beam plane to restrict the illumination of the crystal by the incident beam to the section shown.

Table 3. *Results for a 100-sided 'cylinder' with $\mu = 1$ and cross-sectional area π*

2θ (°)	T	$\bar{T}$	Estimated error
0.0	0.196426	1.54521	0.15D−14
10.0	0.197136	1.53674	0.31D−14
20.0	0.199257	1.51192	0.32D−14
30.0	0.202740	1.46283	0.35D−14
40.0	0.207479	1.42271	0.34D−14
50.0	0.213318	1.36530	0.23D−14
60.0	0.220072	1.30412	0.22D−14
70.0	0.227537	1.24210	0.27D−14
80.0	0.235506	1.18148	0.21D−14
90.0	0.243676	1.12380	0.23D−14
100.0	0.252111	1.07010	0.46D−14
110.0	0.260326	1.02104	0.26D−14
120.0	0.268194	0.977019	0.27D−14
130.0	0.275491	0.938388	0.40D−14
140.0	0.281984	0.905481	0.29D−14
150.0	0.287429	0.878735	0.27D−14
160.0	0.291577	0.858734	0.22D−14
170.0	0.294195	0.846212	0.27D−14
180.0	0.295093	0.841916	0.22D−14

Table 4. *Results for a 74-sided 'sphere' with $\mu = 1$ and volume $4\pi/3$*

2θ (°)	T	$\bar{T}$	Estimated error
0.0	0.242502	1.324673	0.39D−15
10.0	0.243651	1.315127	0.18D−14
20.0	0.245721	1.297254	0.34D−14
30.0	0.248635	1.271872	0.28D−14
40.0	0.252576	1.238634	0.48D−14
50.0	0.257941	1.196774	0.58D−14
60.0	0.264163	1.151518	0.38D−14
70.0	0.270824	1.105970	0.33D−14
80.0	0.277754	1.061313	0.36D−14
90.0	0.284869	1.018334	0.39D−14
100.0	0.292952	0.973514	0.27D−14
110.0	0.300783	0.932658	0.28D−14
120.0	0.308085	0.896306	0.15D−14
130.0	0.314671	0.864821	0.15D−14
140.0	0.320520	0.837873	0.20D−14
150.0	0.325753	0.814643	0.13D−14
160.0	0.329687	0.797323	0.18D−14
170.0	0.331969	0.787025	0.18D−14
180.0	0.332457	0.784443	0.58D−15

on the rotation of the multifaceted cylinder about its axis. The values given in *International Tables for X-ray Crystallography* (1959) are only in general agreement with Table 3.

The 74-sided sphere is modelled with faces {100}, {110}, {111} and {*pqr*}, where (*pqr*) makes equal angles with (100), (110) and (111). Results are shown in Table 4. As expected, the accuracy of representing a true sphere is not as good as the accuracy achieved by the polycylinder but is more than adequate for practical purposes. The figures given for scattering angles 0 and 180° may be compared with the exact results for a perfect sphere with $\mu R = 1$, which are $T_0 = 0.242\,493$ and $T_{180} = 0.332\,418$. The calculation for each 2θ value took approximately 3 to 5 s on the Sun Sparc 10 CPU.

Concluding remarks

It has been shown in this paper that a fast accurate calculation of the transmission factor can be made by

combining the formalism originally proposed by de Meulenaer & Tompa (1965) and subsequently developed by Alcock (1970) and by Blanc, Schwarzenbach & Flack (1991) with the more general analysis made by Clark (1993). It is slightly ironic that the simplest equation to use for calculating the transmission factor [equation (9)] turns out to be one that could have been very easily derived by converting the volume integrals into surface integrals by the use of Gauss's theorem and then using de Meulenaer & Tompa's formula [equation (12)] applied to a plane area to perform the surface integrals. This procedure avoids the subdivision of polyhedra into tetrahedra, replacing it with the much easier subdivision of polygons into triangles.

In addition to the mathematical development, this paper has outlined an algorithm that speeds up the searches for the vertices of the Howells polyhedra significantly. A detailed description of the program will be submitted to *Computer Physics Communications*. We note that with this program it is feasible to study crystals with 100 faces or more. A significant addition, too, is the automatic calculation of the estimated error in the calculation. This allows ready identification of the special crystal configurations that give numerical inaccuracies. On a multifaceted crystal, it is impossible to predict when these might occur but, as a very small change in the configuration usually eliminates the errors, they are easy to correct.

Finally, we have presented test results to a higher accuracy than previously given in the literature. We believe these will be useful both to those already using absorption correction programs and to those who may develop new code in future.

APPENDIX 1

The ordering of a set of planes round a vertex is based on the observation that any three non-coplanar vectors **a**, **b**, **c** form a right-handed set if the triple scalar product $[\mathbf{a}, \mathbf{b}, \mathbf{c}]$ is positive. This can be extended to N non-coplanar vectors $\mathbf{n}_1, \mathbf{n}_2, \mathbf{n}_3, \ldots, \mathbf{n}_N$. These will be ordered if $[\mathbf{n}_i, \mathbf{n}_j, \mathbf{n}_k] > 0$ for all i, j, k in the range $[1, N]$ and $i < j < k$.

While such an order must exist for any three non-coplanar vectors, it does not have to exist for any N vectors where $N > 3$. However, if the $\mathbf{n}_i$ are normals to a set of planes that pass through a common point, then the existence of such an order implies that the set of planes will have a common included region beneath them. If there is no single pair ($\mathbf{n}_1$, $\mathbf{n}_2$ say) for which $[\mathbf{n}_1, \mathbf{n}_2, \mathbf{n}_k]$ is positive for all $k > 2$ then there is no included region beneath that set of planes.

Difficulties arise when there exist planes that are tangent to the included volume, in the sense that they pass through the vertex, but every point on them apart from the vertex is excluded by another plane (see Fig. 6). In this case, it will be impossible to find a consistent order for the planes. However, it will be possible to find an initial neighbouring pair of planes, 1 and 2, such that $[\mathbf{n}_1, \mathbf{n}_2, \mathbf{n}_k]$ is positive for all $k > 2$. If subsequent attempts to find an ordered set requires some $\mathbf{n}_k$ to be placed between $\mathbf{n}_1$ and $\mathbf{n}_2$ then plane k can be identified as a tangent plane. An example using the planes illustrated in Fig. 6 is that both $[\mathbf{n}_1, \mathbf{n}_2, \mathbf{n}_3]$ and $[\mathbf{n}_1, \mathbf{n}_2, \mathbf{n}_4]$ will be positive, establishing planes 1 and 2 as a neighbouring ordered pair. However, $[\mathbf{n}_1, \mathbf{n}_3, \mathbf{n}_4]$ will be negative, indicating that the order should be 1, 2, 4, 3. A check of $[\mathbf{n}_2, \mathbf{n}_4, \mathbf{n}_3]$, however, will show that this is also negative and hence plane 4 is a tangent plane. Similar considerations apply to planes that are tangent to an edge rather than a vertex (Clark, 1993).

APPENDIX 2
Small a or μ

For completeness, we give the expansions required for T and $\overline{T}$ in the small a or μ cases. In both cases, we need to evaluate

$$F(a,\mu) = a^{-1}\{[\psi_1/(L_1 - L_2)(L_1 - L_3)] + [\psi_2/(L_2 - L_1)(L_2 - L_3)] + [\psi_3/(L_3 - L_1)(L_3 - L_2)]\},$$

where for T we have

$$\psi(L) = (-\mu)^{-3}\exp(-\mu L)$$

and for $\overline{T}$

$$\psi(L) = (-\mu)^{-4}(\mu L + 3)\exp(-\mu L)$$

and $L = \mathbf{a} \cdot \mathbf{r} + c$.

Define ω by $\mathbf{a} \cdot \mathbf{r} = a\omega$. Then re-expressing $F(a, \mu)$ in terms of ω and expanding in a Taylor series about

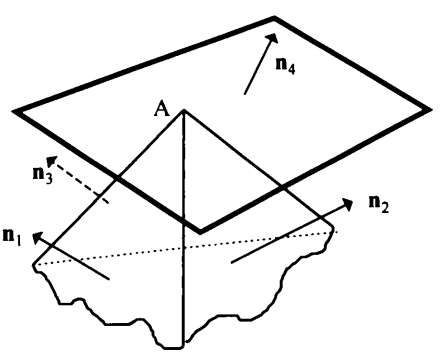

Fig. 6. Except for point A, all points on the tangent plane (plane 4) are excluded by planes 1, 2 or 3.

$a\mu = 0$ gives the required expansion in each case. For T,

$$F(a,\mu) = \exp(-\mu c) \sum_{n=1}^{\infty} [(-a\mu)^{n-1}/(n+2)!] \times S_n(\omega_1, \omega_2, \omega_3),$$

and for $\overline{T}$,

$$F(a,\mu) = \exp(-\mu c)\{\tfrac{1}{6}cS_1(\omega_1,\omega_2,\omega_3) + a \sum_{n=2}^{\infty} [(-a\mu)^{n-2}/(n+2)!](-\mu c + n - 1) \times S_n(\omega_1,\omega_2,\omega_3)\}.$$

In these expressions, $S_n(\omega_1, \omega_2, \omega_3)$ is the fully symmetric function of order n of three variables; *i.e.* $S_1 = \omega_1 + \omega_2 + \omega_3$, $S_2 = \omega_1^2 + \omega_2^2 + \omega_3^2 + \omega_1\omega_2 + \omega_3\omega_1 + \omega_2\omega_3$ *etc.* S_n can be generated rapidly for any n by using the simple algorithm $S_n = \omega_3 S_{n-1} + T_n$, $T_n = \omega_2 T_{n-1} + U_n$, $U_n = \omega_1 U_{n-1}$ with $S_0 = T_0 = U_0 = 1$.

References

ALCOCK, N. W. (1970). *Crystallographic Computing*, edited by F. R. AHMED, pp. 271–278. Copenhagen: Munksgaard.

ALCOCK, N. W. (1974). *Acta Cryst.* A**30**, 332–335.

BLANC, E., SCHWARZENBACH, D. & FLACK, H. D. (1991). *J. Appl. Cryst.* **24**, 1035–1041.

BRAIBANTI, A. & TIRIPICCHIO, A. (1965). *Acta Cryst.* **19**, 99–103.

BUSING, W. R. & LEVY, H. (1957). *Acta Cryst.* **10**, 180–182.

CAHEN, D. & IBERS, J. A. (1972). *J. Appl. Cryst.* **5**, 298–299.

CLARK, R. C. (1993). *Acta Cryst.* A**49**, 692–697.

FLACK, H. D., VINCENT, M. G. & ALCOCK, N. W. (1980). *Acta Cryst.* A**36**, 682–686.

HOWELLS, R. G. (1950). *Acta Cryst.* **3**, 366–369.

International Tables for X-ray Crystallography (1959). Vol. II, pp. 291–305. Birmingham: Kynoch Press. (Present distributor Kluwer Academic Publishers, Dordrecht.)

MEULENAER, J. DE & TOMPA, H. (1965). *Acta Cryst.* **19**, 1014–1018.

REID, J. S. (1993). *Acta Cryst.* A**49**, 190–198.

SCHWARZENBACH, D. & FLACK, H. D. (1989). *J. Appl. Cryst.* **22**, 601–605.

SCHWARZENBACH, D. & FLACK, H. D. (1992). *J. Appl. Cryst.* **25**, 69.

ZACHARIASEN, W. H. (1967). *Acta Cryst.* **23**, 558–564.

Acta Cryst. (1995). A**51**, 897–902

Rapid Suppression and Modulation of the Diffracted Beam in a Single Crystal Excited by Ultrasound

BY E. M. IOLIN

Institute of Physical Energies of the Latvian Academy of Sciences, 21 Aizkraukles Street, Riga, LV-1006, Latvia

(*Received* 13 *September* 1993; *accepted* 22 *May* 1995)

Abstract

The results of a theoretical analysis of the influence of a high-frequency standing acoustic wave on the angular spectrum of a diffracted beam in a perfect crystal are presented. The rapid suppression and modulation of the intensity at the center of the diffraction pattern are found for the first time. The characteristic duration of this modulation is many times smaller than the period of the acoustic wave. These effects can be used for the suppression and modulation of a highly collimated monochromatic beam of synchrotron radiation.

Introduction

The influence of the acoustic waves (AW) on the diffraction of X-rays and thermal neutrons in single crystals has been considered by many authors (*e.g.* Spencer & Pearman, 1970). Depending on the ultrasonic AW frequency, a distinction can be made between two different mechanisms. At $k_s \ll \Delta k_0$ ($\Delta k_0 = 2\pi/\tau$, τ is the extinction length, k_s is the wave vector of the AW), the ultrasound deformations simply expand (in general) the Bragg-angle scattering interval [for a more detailed analysis see Kulda, Vrana & Mikula (1988), Lukas & Kulda (1989), Mikula, Lukas & Kulda (1992)]. A high-frequency ultrasonic AW with $k_s > \Delta k_0$ mixes the states corresponding to the different sheets of the dispersion surface (Köhler, Möhling & Peibst, 1974). Such a mixing leads to a number of effects, *e.g.* resonant suppression of the Borrmann effect (Entin, 1977), a new *Pendellösung* determined by AW (Iolin & Entin, 1983); Entin & Puchkova, 1984; Iolin, Zolotoyabko, Raitman, Kuvaldin & Gavrilov, 1986). In general, AW increases the integral intensity I_h of the diffracted beam in perfect crystals and leads to decreasing I_h in slightly deformed single crystals (Iolin, Raitman, Kuvaldin & Zolotoyabko, 1988).